OCEANOGRAPHY

Oxygen supersaturation protects coastal marine fauna from ocean warming

Folco Giomi[1]*†, Alberto Barausse[2], Carlos M. Duarte[1], Jenny Booth[1], Susana Agusti[1], Vincent Saderne[1], Andrea Anton[1], Daniele Daffonchio[1], Marco Fusi[1]*†‡

Ocean warming affects the life history and fitness of marine organisms by, among others, increasing animal metabolism and reducing oxygen availability. In coastal habitats, animals live in close association with photosynthetic organisms whose oxygen supply supports metabolic demands and may compensate for acute warming. Using a unique high-frequency monitoring dataset, we show that oxygen supersaturation resulting from photosynthesis closely parallels sea temperature rise during diel cycles in Red Sea coastal habitats. We experimentally demonstrate that oxygen supersaturation extends the survival to more extreme temperatures of six species from four phyla. We clarify the mechanistic basis of the extended thermal tolerance by showing that hyperoxia fulfills the increased metabolic demand at high temperatures. By modeling 1 year of water temperatures and oxygen concentrations, we predict that oxygen supersaturation from photosynthetic activity invariably fuels peak animal metabolic demand, representing an underestimated factor of resistance and resilience to ocean warming in ectotherms.

INTRODUCTION

Ocean warming affects the life history and fitness of marine organisms (*1*). Experimental evidence indicates that as temperatures rise above thermal optima, oxygen threshold (as % saturation) for hypoxemia rises as a consequence of the steep increase in respiratory demand [(*2*–*4*), but see also (*5*)]. Thus, oxygen availability in aquatic habitats may represent a major threat for ectothermal species since it is tightly connected to the capacity to endure warming and thermal stress and ultimately affects organismal survival (*2*–*7*).

The possibility to maintain an effective aerobic performance, i.e., the capacity to fulfill metabolic oxygen demand, is the key requirement for ectotherm animal species to preserve their energy balance and survive and avoid fitness reduction under warming (*3*, *6*–*9*). Experimentally resolved thermal limits of marine fauna have demonstrated the risk of catastrophic mortality with ocean warming and marine heat waves (*10*). However, photosynthetic activity in coastal habitats can provide an extra oxygen supply that may enhance animal aerobic performance under warming, a possibility that has not yet been considered. Here, we show a clear coupling between diel changes in water temperature and dissolved oxygen in vegetated coastal habitats in the Red Sea and experimentally demonstrate that hyperoxia during the warmest hours of the day enhances the survival scope of marine animals under high to extreme water temperatures.

RESULTS AND DISCUSSION

The Red Sea is the warmest sea on Earth, with mean maximum summer temperatures up to 32°C and warming rates faster than the global ocean average (*11*). Using a unique high-frequency monitoring dataset of dissolved oxygen concentration and water temperature, at 5-min intervals, in seagrass meadows, coral reefs, and mangrove stands, the three most prevalent biogenic coastal habitats in the Red Sea, we recognized a marked diel cycle, with daytime oxygen increase in phase with temperature increase (Fig. 1). This positive correlation is due to photosynthetic oxygen release during the day (Fig. 1B and fig. S1), promoted by light availability and warm water, and oxygen consumption through community respiration at night synchronized with temperature decline. This finding shows that biological processes control oxygen concentration in these coastal waters, outweighing the decline of oxygen solubility with increasing temperature. In a cross-correlation analysis, the relationship between detrended time series of water temperature and lagged dissolved oxygen concentration was highest at zero-time lag for mangroves and coral reefs (Pearson $r = 0.58$ and 0.70, respectively; $P < 0.001$) and at a 10-min lag for seagrass meadows ($r = 0.60$, $P < 0.001$). Thus, the daily fluctuations of the two time series are in nearly synchronous phase, with peaks of water temperature matching the time of maximum dissolved oxygen concentration (Fig. 1, and see also figs. S2 and S3). This phenomenon is not restricted to tropical habitats, since daytime photosynthetic oxygen enrichment during summer also occurs at temperate (*12*) and polar latitudes (*13*), revealing the potential occurrence of diel oxygen supersaturation in coastal habitats at a global scale.

We experimentally tested ectotherm animal sensitivity to warming under ecologically relevant conditions in six common marine species living in mangroves, seagrass meadows, and coral reefs (fig. S2). In all species, exposure to experimentally induced oxygen supersaturation (140 ± 3% of oxygen saturation), mimicking the environmental conditions that they regularly experience when water is warm, consistently enhanced lethal heat thresholds, extending their survival under extreme temperatures (Fig. 2). When the animals, which spanned four different phyla, were exposed to oxygen supersaturation, the 50% lethal temperature (LT_{50}) increased by 1° to 4°C, depending on the species, with respect to that under normoxia (97 ± 2% of oxygen saturation). Levels of oxygen supersaturation comparable to those observed in the habitats examined (Fig. 1) significantly enhanced animal survival, contributing to explain the persistence and endurance of organisms in aquatic habitats under extreme temperatures.

To build a mechanistic understanding of this unexpected thermal tolerance, we investigated the sublethal physiological performance of the mangrove inhabitant spiny rock crab, the portunid *Thalamita crenata*

[1]King Abdullah University of Science and Technology (KAUST), Red Sea Research Center (RSRC), Thuwal 23955-6900, Saudi Arabia. [2]Department of Biology, University of Padova, via U. Bassi 58/b, 35131 Padova, Italy.
*Corresponding author. Email: folcog@gmail.com (F.G.); marco.fusi@kaust.edu.sa (M.F.)
†These authors contributed equally to this work.
‡Present address: School of Applied Sciences, Edinburgh Napier University, Sighthill Campus, Edinburgh, UK.

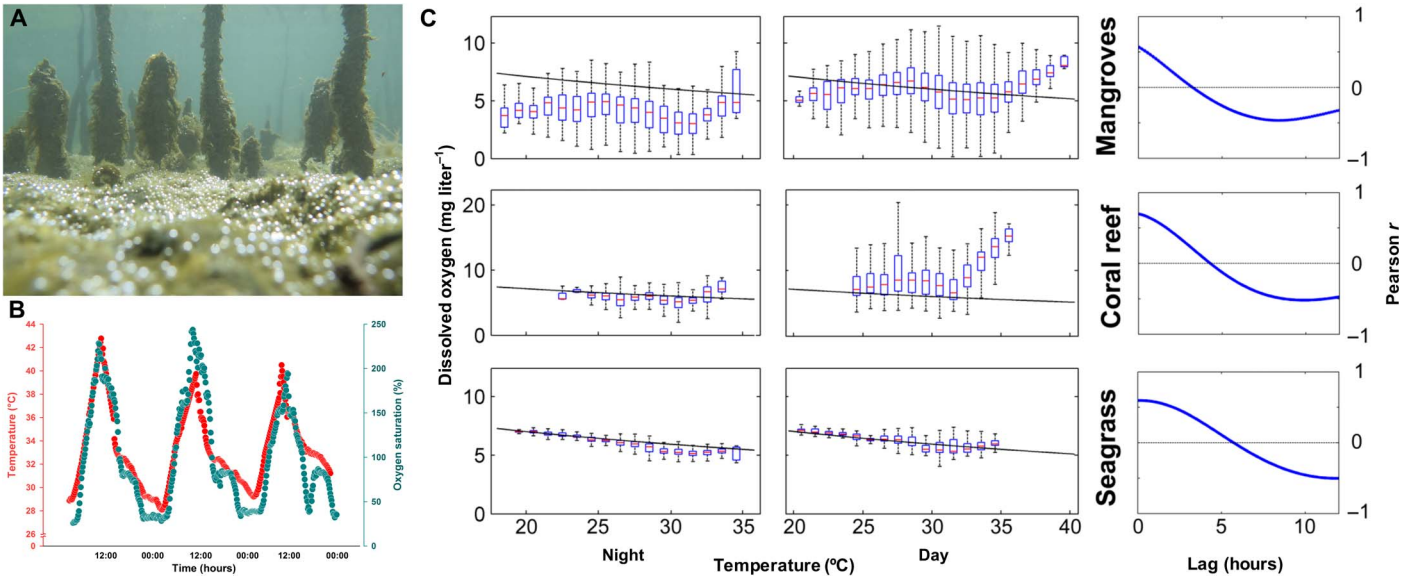

Fig. 1. Dissolved oxygen concentration and water temperature in Red Sea coastal habitats. (**A**) Oxygen production in a mangrove forest floor colonized by a photosynthetic biofilm formed by cyanobacteria, algae, and microphytobenthos that are producing oxygen bubbles during daytime (10:30 a.m., 12 May 2018). Production is enhanced by the warm temperature. In the picture, the colonization of the mangrove tree pneumatophores by this biofilm can also be appreciated. Photo credit: Marco Fusi, King Abdullah University of Science and Technology (KAUST). (**B**) Example of diel seawater temperature and dissolved oxygen fluctuations, with peaks of oxygen production during the hottest hours that determine local hyperoxic conditions. These data were collected in the mangrove environment during September 2017. (**C**) Dissolved oxygen concentration and water temperature in the three dominant coastal habitats of the Red Sea between August–September 2016 and August 2017. Oxygen concentration is plotted for 1°C temperature intervals during nighttime or daytime: The box edges enclose the first and third quartiles of the observations, the red line is the median, the whiskers encompass 99.3% of the observations (outliers were omitted for clarity of reading), and the black line shows the oxygen concentration at saturation in seawater (left and center). The cross-correlations between water temperature and lagged dissolved oxygen concentration (right), detrended to analyze the oscillations during the day, show that the two time series are in phase (the Pearson correlation coefficient is highest at zero lag for mangroves and coral reefs and at a 10′ lag for seagrass).

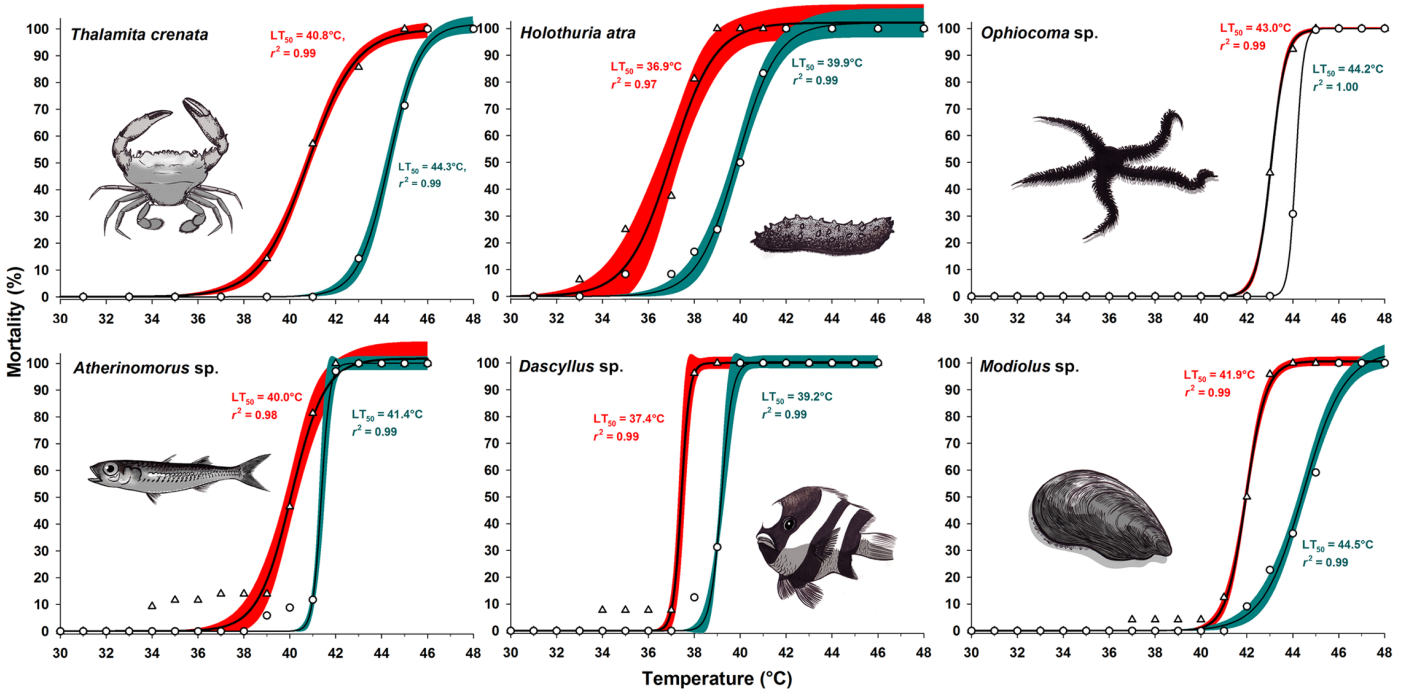

Fig. 2. Experimental relationship between water temperature and mortality for six marine species under simulated conditions of habitat normoxia (triangles) and hyperoxia (circles). The filled areas represent the 95% confidence intervals (normoxia: red; hyperoxia: cyan) for each three-parameter sigmoid regression (black line). The LT_{50} of the organisms and R^2 for each regression are reported in the figure in red (normoxia, 97 ± 2% of oxygen saturation) or cyan (hyperoxia, 140 ± 3% of oxygen saturation). Temperature ramping was 1°C every 30 min to mimic the daily environmental warming rates. The symbols can hide data points. Animal illustration credit: Allende Bodega Martinez.

Rüppell 1830, under these empirically resolved oxygen regimes. Our measurements of basal metabolic response to acute warming demonstrate that the diel phenomenon of oxygen supersaturation supports the aerobic performance of marine fauna and reveals an unrealized potential for enhancing their thermal tolerance (Fig. 3A). Similarly, to the mortality threshold, oxygen supersaturation raised the critical heat limit for aerobic respiration, defined as the temperature above which oxygen consumption is no longer sustained (*2*). This increment of critical thermal limit from 38° to 40°C exceeds the maximum temperature recorded in the field (39.2°C for mangroves), providing a safe margin for the species persistence during heat peaks. Furthermore, the beneficial effect of oxygen supersaturation was not limited to extreme temperature tolerance, but it enhanced the overall aerobic performance of crabs during warming in daytime. The basal oxygen consumption rate did not differ between normoxia and hyperoxia at intermediate temperatures (20° to 30°C), while with the further warming, the temperature-induced increase of metabolic demand becomes suddenly unsustainable under normoxic conditions since oxygen requirement exceeds the amount of oxygen that crabs can extract from the water (Fig. 3A). The increased metabolic demand peaks at the highest temperatures (36° to 40°C), where oxygen supersaturation (Fig. 1) fuels a steady consumption rate higher than that occurring in normoxia, where the consumption rate is critically limited by oxygen availability [generalized additive model (GAM); $F_{1,1} = 5.451$, $P < 0.05$] (Fig. 3A).

This finding becomes ecologically relevant given the natural occurrence of high temperatures in the central Red Sea that, particularly in the mangrove stand, approach the upper lethal threshold experienced by ectotherm animals under normoxic conditions. Oxygen supersaturation conditions, which favor an enhanced thermal performance, were common in the coastal habitats of the central Red Sea monitored, encompassing 25.3, 50.3, and 33.4% of the observational period in mangroves, coral reefs, and seagrass meadows, respectively. These results validate, at the ecosystem scale, laboratory evidence of the benefit of hyperoxic regimes on ectotherm thermal tolerance for different taxa, such as Antarctic fishes (*14*) or freshwater crustaceans (*15*).

Our results demonstrate that diel oxygen supersaturation supported by photosynthetic activity is exploited by animals to fuel increased metabolic demands under high to extreme temperatures and to potentially sustain their survival under episodic heat waves. These findings provide evidence of a previously unrecognized mechanism of resistance of marine fauna in close association with productive vegetated coastal habitats to acute temperature fluctuations, reframing our understanding of coastal species' vulnerability to ocean warming.

The positive effects generated by photosynthetic activity are evident during daytime when oxygen supersaturation boosts the thermal tolerance of marine fauna. Conversely, the benefits of the association of animals with algae and plants are less evident during the night when photosynthesis stops and primary producers become competitors for dissolved oxygen, potentially driving local conditions of acute hypoxia. In the mangrove stand, for example, oxygen concentration was below 50 and 10% of saturation for 18.1 and 0.3% of the observational period, respectively. To investigate this issue, we experimentally quantified two physiological processes related to hypoxia: the onset of critical low oxygen pressure (PO_2crit) (*16*) and the capacity of recovery from temporary oxygen depletion. We measured a significantly lower PO_2crit in crabs that had experienced oxygen supersaturation with respect to normoxia ($F_{1,10} = 14.028$, $P < 0.05$) (Fig. 3B). In addition, crabs previously exposed to hyperoxic water conditions were able to oxyregulate down to 38.2 mmHg, but only down to 73.4 mmHg for those crabs previously exposed to normoxic water. This indicates that temporary hyperoxic exposure extends the oxyregulating capacity down to relatively low oxygen concentrations. Similarly, oxygen supersaturation enables a rapid and efficient recovery from acute hypoxic episodes (Fig. 3C), such as those occurring during the night in productive habitats. After being exposed for 15 hours to hypoxia (10% of water oxygen saturation), animals presented an average (±SE) of 15.5 ± 1.85 mM lactate in the hemolymph. By subsequently exposing the hypoxia-stressed animals to hyperoxia or normoxia, we measured a significantly faster recovery to the normal lactate hemolymph concentrations for the animals under hyperoxia [generalized linear model (GLM); $F_{1,36} = 68.54$, $P < 0.0001$]. The amount of lactate (i.e., the principal end product of anaerobic metabolism in crustaceans) accumulated in the hemolymph was completely depleted within a short time when the organism had the possibility to recover from the oxygen debt under hyperoxia, while the

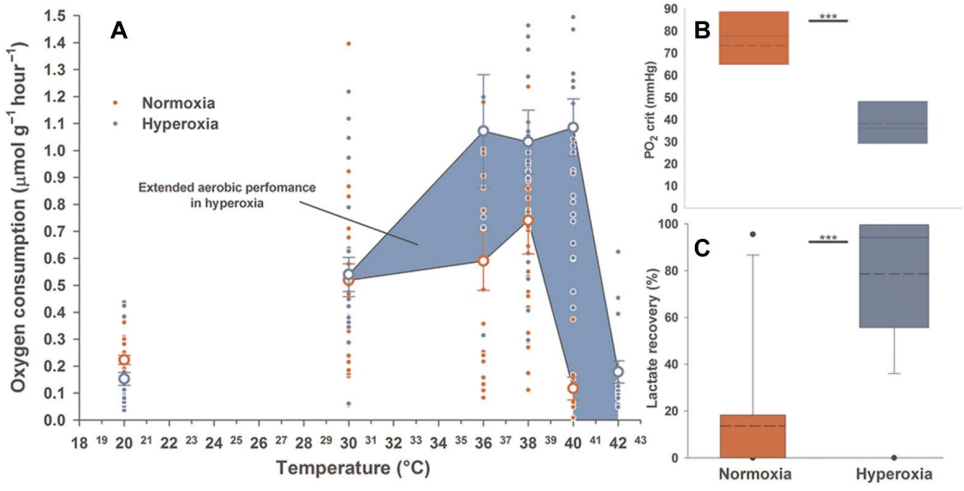

Fig. 3. Physiological performances of *T. crenata* under simulated conditions of habitat normoxia (red) and hyperoxia (cyan). (**A**) Metabolic thermal response; the light blue area indicates the extended aerobic performance, red and cyan dots represent individual measurements, and the empty circles are the means ± SE ($n = 24$). (**B**) Critical PO_2. (**C**) Lactate recovery. The asterisks in (B) ($n = 7$, $P < 0.05$) and (C) ($n = 19$, $P < 0.0001$) indicate statistically significant differences between the two groups tested.

recovery process was slower under normoxia. These experiments show that diel oxygen supersaturation not only extends the animal heat tolerance window in coastal ecosystems but also enhances their resistance and resilience to acute hypoxic events, such as those occurring during the night.

Projecting laboratory-derived aerobic performances onto the environmental conditions of the mangrove stand where *T. crenata* was collected, we predict that, over the course of a year, crabs frequently experience a combination of high temperatures and oxygen supersaturation, resulting in intense oxygen consumption rates (Fig. 4). Invariably, the enhanced thermal performance of the animals is fueled by oxygen concentrations largely exceeding oxygen water saturation during peak metabolic demand. Our predictions link large diel environmental variations in coastal habitats to the high plasticity of aerobic performance in aquatic fauna. This mechanistic framework contributes to explain the persistence and performances of ectotherm species in habitats characterized by marked oscillations in water temperature and oxygen availability, where benthic primary producers grow.

Organisms that inhabit coastal environments, which reach high temperatures during the daytime, would therefore benefit from the thermal refugia offered by highly productive habitats. Where a mosaic of environments is available, vulnerable fauna may seek the shelter offered by the hyperoxic conditions in seagrass meadows, coral reefs, algal stands, and/or highly productive microbial mats associated with mangroves. While we only assessed responses of adult stages, hyperoxia associated with the high photosynthetic activity of algae, such as that occurring in tidal pools, has also been reported to accelerate development time and success in eggs of benthic invertebrates (*17*). Hence, the benefits of hyperoxia may accumulate throughout the entire life history of the organisms and provide an additional explanation for the role of these highly productive vegetated habitats as favorable spawning and recruitment habitat, beyond their role in providing food and shelter from predators (*18*). This essential ecological service is another contribution of vegetated habitats to the mitigation of global warming and ocean acidification through carbon sequestration (*19*, *20*), provision of nursery sites for animal species (*21*), defense against coastal erosion (*22*), and protection from pathogens (*23*).

The significance of oxygen supersaturation becomes even more relevant in the light of climate change, considering that hypoxic zones due to dystrophic events are now more frequent and spread around coastal areas (*24*). Our study points out that the effective conservation and restoration of autotrophic coastal habitats is fundamental to support the resistance of associated coastal marine fauna to global warming.

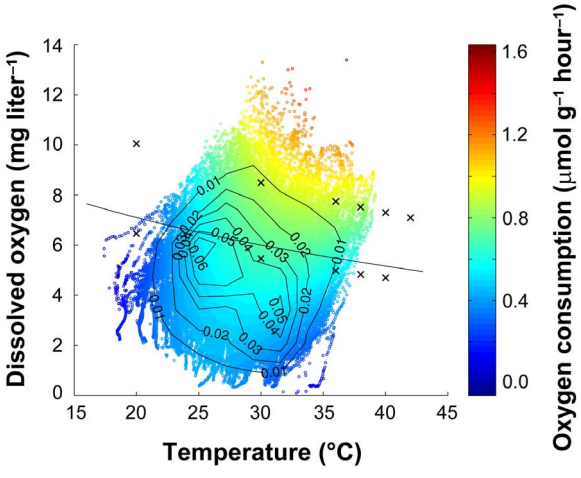

Fig. 4. Oxygen consumption of *T. crenata* projected from dissolved oxygen and water temperature measured in a mangrove stand of the Red Sea. The dots represent observations made every 5 min between August 2016 and August 2017, and colors indicate the oxygen consumption predicted using the best model (R^2 = 0.55) fitted to laboratory measurements, indicated by *x*. The black line indicates the air-saturation oxygen concentration in water. Black isocurves link locations in the plot with the same density of observations (as indicated in relative units by the isoline labels), i.e., locations around which a similar number of records were observed; see Materials and Methods for more details. The highest metabolic performances occur at high temperature and under oxygenation conditions that largely exceed air saturation. This enhanced thermal performance can be fueled by oxygen supersaturation in the habitat.

MATERIALS AND METHODS

Environmental data logging

The mooring of multiparametric probes equipped with calibrated conductivity, water temperature, depth, and dissolved oxygen concentration (optical) sensors (CTD-O_2) (Exosond 2,YSI Inc., Yellow Springs, USA) was performed in a fringe mangrove forest, a seagrass-dominated coastal lagoon, and a coral barrier reef on the Red Sea nearshores from August/September 2016 to August 2017 (mangroves: 17 August 2016 to 19 August 2017; coral reef: 31 August 2016 to 22 August 2017; seagrasses: 06 September 2016 to 22 August 2017). One probe was deployed in each habitat, where it was firmly attached to a frame (*25*, *26*). The logging frequency was 5 min, except for the mangroves in the period before November 2016 when observations were available every 10 min (the results of the statistical analyses did not change when repeating all analyses for mangroves by assuming that, before November 2016, each missing observation due to the lower sampling frequency was equal to the immediately preceding valid observation, thus achieving a 5-min sampling frequency).

The probes were located at the transition between the benthic boundary layer and the open water, in close proximity to the biogenic habitats to better assess the influence of in situ metabolic activity on environmental parameters. In the mangroves, the probe was moored on the seaward fringe (22°20′21″N, 39°05′20″E) under the canopy of the trees, measuring at approximately 5 cm above the sediment. In the coastal lagoon (22°23′23.2″N, 39°08′07.9″E), the probe was moored within the canopy of an *Enhalus acoroides* seagrass meadow, with the sensors located approximately 50 cm above the sediment, close to the top of the seagrass canopy. In the coral reef, the probe was attached vertically to a coral wall on the back reef side (22°15′03.7″N, 38°57′49.3″E), and the sensors were measuring approximately at 5 cm from the reef top.

To provide support to the data retrieved by the probes, we also deployed PME miniDOT Dissolved Oxygen Loggers at 1 to 2 cm from the sediment surface as close as possible to the habitat the species tested experienced (fig. S2). Data retrieved by the miniDOT loggers showed the same pattern of oxygen and temperature detected by the probes (fig. S3).

Animal lethal responses

To characterize the potential of oxygen supersaturation in shaping the thermal tolerance of marine ectotherms and to demonstrate the generality of this framework, we sampled six species spanning four different phyla. In detail, 14 individuals of *T. crenata* (Arthropoda: Portunidae) and 77 of *Atherinomorus* sp. (Chordata: Atherinidae) were collected from the mangrove stand around King Abdullah University of Science

and Technology (KAUST) at the "Ibn Sina" field research station (22°20′19.90″N, 39°5′24.30″E); 28 individuals of *Holoturia atra* (Echinodermata: Holothuroidae) and 58 individuals of *Dascyllus* sp. (Chordata: Pomacentridae) were collected in the coral reef near Rabigh (22°20′19.90″N, 39°5′24.30″E); 26 individuals of *Ophiocoma* sp. (Echinodermata: Ophiocomidae) and 46 individuals of *Modiolus* sp. (Mollusca: Mytilidae) were collected in KAUST at the Ibn Sina field research station. We immediately transferred the animals to the aquarium facilities at KAUST and let them recover from the handling stress for 24 hours in filtered, normoxic seawater (salinity 40 ppt, 20°C) without feeding them. Temperature-induced mortality rate and LT_{50} were measured following the method described by Giomi and colleagues (*27*). In detail, for each species, two groups of individuals underwent different treatments: Half of the animals were exposed to normoxic (97 ± 2% of oxygen saturation) and half to hyperoxic (140 ± 3% of oxygen saturation) conditions for 2 hours before the start of a temperature ramping of 1°C every 30 min, mimicking environmental temperature fluctuations. Oxygen concentration was monitored during the entire experiment using a calibrated multiparametric probe (SevenGo Duo Pro SG98 Portable RDO/pH/Ion Meter, Mettler Toledo Instruments) and adjusted to maintain supersaturation by regulating the flow of air and nitrox (O_2 at 36%). The mortality of individuals (defined through the nonreactivity to tactile stimulus) was assessed every 30 min. Dead individuals were immediately removed from the experimental tank, and the experiments were terminated when all animals were dead.

This project was completed under the Saudi Arabia and KAUST ethics permit (Institutional Animal Care and Use Committee approval 18IACUC10).

Animal sublethal physiological responses

As the experimental species to investigate the effect of oxygen supersaturation on ectotherm thermal response, we selected *T. crenata*, one of the most widespread crabs throughout the Indo-Pacific and Red Sea coastal waters, inhabiting mangroves, saltmarshes, seagrasses, and rocky shores (*28*–*30*). It represents a keystone species in intertidal habitats due to its predatory role (*31*) and an interesting model to study thermal tolerance because it inhabits the shallow water of coastal habitats (*28*). We collected a total of 114 males with similar carapace width (about 55 ± 7 mm) from the mangrove stand around KAUST. We immediately transferred them to the aquarium facilities and let them recover from handling stress for 24 hours in normoxic filtered seawater (salinity 40 ppt, 20°C), following the procedures described by Fusi and colleagues (*32*), without feeding them. In the laboratory, the acclimation temperature was set at 20°C to mimic the field temperature during the nighttime when animals were collected. A total of 48 animals were randomly selected for metabolic measurement (MO_2), 14 for the critical PO_2 experiment and 38 were used for the lactate measurement. The first two groups of crabs were allowed to recover directly in the respiratory chambers to minimize handling stress. Experiments to measure MO_2 were then performed starting at 20°C and ramping temperature with a 1°C increase every 30 min, mimicking the diel warming rate of seawater (*33*).

Oxygen consumption (MO_2)

Rates of oxygen consumption at rest (MO_2) were measured in intermittent flow Perspex respirometric chambers (customized by JEMITEC Technische Komponenten, Garlstor, Germany; 500-ml volume) keeping 24 animals at normoxia and 24 at hyperoxia. MO_2 was measured using an oxygen sensor spot (Sensor Type PSt3 PreSens, Regensburg, Germany), glued to the inside wall of the chamber and connected to a single-channel oxygen transmitter Fibox (Microx) 4 (PreSens, Regensburg, Germany) through an optical fiber. No spontaneous activity was noticed during the measurements. For each oxygen treatment, we increased temperature at 1°C steps (obtained with the control of the water bath; GP 200, Grant Instruments, Cambridge, UK) every 30 min and measured MO_2 at seawater temperatures of 20°, 30°, 38°, 40°, 42°C. Each measurement was carried out during the final 5 min of the 30-min step by closing the respiratory chambers, and the oxygen saturation never decreased by more than 5% of the value of the corresponding treatment.

Following the procedure used by Fusi *et al.* (*32*), for each measurement, we kept two chambers empty as controls to assess the microbial oxygen consumption at the temperatures tested. Prior to and after the measurements, all the hoses and tubes, as well as the connectors, were cleaned in alcohol 70% and in bleach 10% and carefully rinsed with sterile Milli-Q water. This treatment ensured the removal of microorganisms. In addition, prior to placing animals in the chambers, we gently cleaned the carapace with sterile seawater to minimize contamination of microbes carried by the animals. At lower temperatures (20° to 30°C), the microbial oxygen consumption was negligible, and at higher temperatures, it was less than 1% of crab consumption. The water used in the experiment was prefiltered seawater to minimize the contamination of microbes.

Lactate concentration

Lactate concentration was measured to evaluate the anaerobic metabolism on which animals rely during hypoxia exposure (*34*), using a Lactate Pro 2 Analyser (www.lactatepro.com.au/) on the hemolymph of the venous blood withdrawn from the sinus below the arthrodial membrane, at the base of the fourth or fifth pereiopod of the crab [see methods in (*35*)]. Lactate was tested in 38 animals exposed to 10% of water oxygen saturation for 15 hours, obtained by flushing nitrogen into the seawater. We then placed 19 animals under normoxia and 19 at hyperoxia, and after 1 hour and 45 min, we remeasured lactate to assess the efficiency of the recovery from lactate accumulation during hypoxia exposure. This measure was made at a constant temperature of 25°C. Water oxygen saturation was monitored using a MiniDOT logger (www.pme.com/products/minidot).

Critical PO_2

Animals inhabiting aquatic habitats may often experience moderate to severe hypoxic conditions, since several ecological factors such as stratification, salinity, temperature, or plant and microbial respiration may reduce oxygen availability (*36*). *T. crenata* naturally experiences fluctuations of oxygen concentration throughout the day, and therefore, we tested the respiration of the animals at progressively lower environmental oxygen pressure (PO_2). With the same experimental setup used to measure MO_2, we determined the critical oxygen pressure (PO_2crit), which represents the lowest oxygen pressure at which an oxyregulator species maintains a constant rate of oxygen consumption. PO_2crit at 20°C was determined on seven animals previously acclimated in normoxia of oxygen saturation and seven previously acclimated in hyperoxia by progressively decreasing oxygen pressure. PO_2crit was calculated as the breakpoint of the graph depicting the PO_2/MO_2 relationship adopting a Piecewise linear regression function (implemented with SigmaPlot v.11).

Statistical analyses

Water temperature and dissolved oxygen

Environmental monitoring observations were assigned to day or night based on the presence or absence of solar radiation (measured in W m^{-2}

every 5 min at the Ibn Sina Field Research Station in KAUST using a CS320 Solar sensor from Campbell Scientific). The multiparametric probe in the mangrove stand was placed in the low intertidal area and occasionally emerged due to tidal oscillations; therefore, in statistical analyses, we used observations made during submersion periods only.

Table S1 reports the number of valid observations of dissolved oxygen concentration and corresponding water temperature available for the three habitats during day and night, for temperature intervals of 1°C. Only temperature intervals containing more than 13 valid observations were shown through box plots in Fig. 1.

Dissolved oxygen concentration at 100% saturation in seawater was calculated according to the solubility formulation of Garcia and Gordon, as recommended by the U.S. Geological Survey (*37*). Oxygen solubility was calculated at standard atmospheric pressure (1 atm) and corrected for the effect of salinity. A pressure correction factor was not applied to oxygen solubility, given that in this study, it was compared to experimental observations made at shallow depths. For each of the six subplots of Fig. 1 (three habitats, day or night) and for Fig. 4, the salinity value chosen to calculate the salinity correction factor was the median of the salinity observations corresponding to the temperature-oxygen observations included in that (sub)plot (Fig. 1: for the mangroves, this value was 41.76 ppt at night and 41.89 ppt at day; for the coral reef, 41.02 ppt at night and 40.80 ppt at day; and for the seagrasses, 43.85 ppt at night and 43.79 ppt at day; Fig. 4: it was 41.82 ppt, i.e., a value close to the salinity of the laboratory experiments whose measurements were displayed in the same figure, which was 40 ppt).

Before calculating cross-correlations in Fig. 1, the time series of water temperature and dissolved oxygen concentration were detrended by subtracting a 24-hour central moving average to focus on daily rather than long-term variability. Cross-correlations between the detrended time series were calculated using the Pearson correlation coefficient and different time lags for dissolved oxygen concentration.

To map field observations of water temperature and dissolved oxygen concentration to oxygen consumption rates in Fig. 4, we fitted different models to the available laboratory measurements. Laboratory measurements (11 observations) consisted of oxygen consumption rates assessed at different water temperatures and oxygen saturation levels (normoxia and hyperoxia), at fixed salinity (40 ppt). This information was used to calculate the actual dissolved oxygen concentration in the 11 laboratory measurements by using the formulation of oxygen solubility (i.e., dissolved oxygen concentration at 100% saturation) of Garcia and Gordon, as recommended by the U.S. Geological Survey (*37*), at standard atmospheric pressure (1 atm) and correcting for the effect of salinity. A pressure correction factor was not applied to oxygen solubility given the shallow depth at which the observations had been made. The resulting dataset (11 observations) was then used to model oxygen consumption rate as a function of water temperature and dissolved oxygen concentration. Given the small sample size, we fitted simple polynomial models with a maximum degree of 2 to the observed oxygen consumption rates, with a maximum of four coefficients to be calibrated; water temperature and dissolved oxygen concentration were the independent variables. We picked up the best model in an adjusted R^2 sense to map the oxygen consumption rate to field observations in Fig. 4. R^2 adjusted for the model residual degrees of freedom, a good indicator of fit quality when comparing nested models, is

$$R^2_{\text{adj}} = 1 - \text{SSE}\cdot(n-1)/(\nu\cdot\text{TSS})$$

where SSE is the sum of squared errors of prediction, TSS is the total sum of squares, n is the number of observations, and ν is $n - p$, where p is the number of fitted model coefficients including the intercept. The best model to predict oxygen consumption rate Q (μmol g^{-1} $hour^{-1}$) as a function of dissolved oxygen concentration DO (mg $liter^{-1}$) and water temperature T (°C) was

$$Q = -1.705 + 0.1711\cdot T - 0.2072\cdot\text{DO} - 0.003477\cdot T^2 + 0.009181\cdot T\cdot\text{DO}$$

(R^2 = 0.55, adjusted R^2 = 0.25)

Isocurves in Fig. 4 were created by dividing the plot into a 10-by-10 grid of equally spaced boxes. The fraction of all the observations in the plot falling inside each box was computed and then used to draw isolines linking locations with the same densities of observations (as indicated in relative units by the isoline labels in Fig. 4), based on the contour function of MATLAB.

Physiological performance

Metabolic differences over increasing temperature (explanatory continuous variable) for the two oxygen conditions (explanatory categorical variable, two levels: hyperoxic, normoxic) were tested using a nonparametric generalized additive model with restricted maximum likelihood [GAM, R package "mgcv"; (*38*)].

A generalized linear mixed model using a quasi-Poisson family error distribution was used to test the difference in the lactate recovery rate (the continuous response variable) for animals exposed to different oxygen saturations (the categorical explanatory variable, fixed and orthogonal, two levels: normoxic and hyperoxic). Each individual ID was considered a random factor in the model to account for paired observations.

After verifying the assumptions of normality and homogeneity of variance (Levene's test, $F_{1,10}$ = 0.57, P = 0.466), we carried out an analysis of variance (ANOVA) considering PO_2crit as the response variable and oxygen level as an explanatory categorical variable with two levels: hyperoxic and normoxic. All the analyses were performed using the R software (*39*).

SUPPLEMENTARY MATERIALS

Supplementary material for this article is available at http://advances.sciencemag.org/cgi/content/full/5/9/eaax1814/DC1

Fig. S1. High-frequency monitoring dataset of dissolved oxygen and water temperature in the three dominant coastal habitats of the Red Sea between August–September 2016 and August 2017.

Fig. S2. This picture shows some of the study species that were active during the middle of the day.

Fig. S3. Diel seawater temperature and dissolved oxygen fluctuations measured with the miniDOT loggers nearby the boundary layer of the seagrass habitat where several animals live, including *H. atra* and *T. crenata* among the other species.

Table S1. Number of valid observations of dissolved oxygen concentration and water temperature during night or day, over temperature intervals of 1°C.

REFERENCES AND NOTES

1. E. S. Poloczanska, C. J. Brown, W. J. Sydeman, W. Kiessling, D. S. Schoeman, P. J. Moore, K. Brander, J. F. Bruno, L. B. Buckley, M. T. Burrows, C. M. Duarte, B. S. Halpern, J. Holding, C. V. Kappel, M. I. O'Connor, J. M. Pandolfi, C. Parmesan, F. Schwing, S. A. Thompson, A. J. Richardson, Global imprint of climate change on marine life. *Nat. Clim. Change* **3**, 919–925 (2013).
2. H. O. Pörtner, A. P. Farrell, Physiology and climate change. *Science* **322**, 690–692 (2008).
3. I. M. Sokolova, M. Frederich, R. Bagwe, G. Lannig, A. A. Sukhotin, Energy homeostasis as an integrative tool for assessing limits of environmental stress tolerance in aquatic invertebrates. *Mar. Environ. Res.* **79**, 1–15 (2012).

4. R. Vaquer-Sunyer, C. M. Duarte, Temperature effects on oxygen thresholds for hypoxia in marine benthic organisms. *Glob. Change Biol.* **17**, 1788–1797 (2011).
5. F. Jutfelt, T. Norin, R. Ern, J. Overgaard, T. Wang, D. J. McKenzie, S. Lefevre, G. E. Nilsson, N. B. Metcalfe, A. J. R. Hickey, J. Brijs, B. Speers-Roesch, D. G. Roche, A. K. Gamperl, G. D. Raby, R. Morgan, A. J. Esbaugh, A. Gräns, M. Axelsson, A. Ekström, E. Sandblom, S. A. Binning, J. W. Hicks, F. Seebacher, C. Jørgensen, S. S. Killen, P. M. Schulte, T. D. Clark, Oxygen-and capacity-limited thermal tolerance: blurring ecology and physiology. *J. Exp. Biol.* **221**, jeb169615 (2018).
6. M. E. Dillon, G. Wang, R. B. Huey, Global metabolic impacts of recent climate warming. *Nature* **467**, 704–706 (2010).
7. P. M. Schulte, The effects of temperature on aerobic metabolism: Towards a mechanistic understanding of the responses of ectotherms to a changing environment. *J. Exp. Biol.* **218**, 1856–1866 (2015).
8. J. F. Gillooly, J. H. Brown, G. B. West, V. M. Savage, E. L. Charnov, Effects of size and temperature on metabolic rate. *Science* **293**, 2248–2251 (2001).
9. H. O. Pörtner, R. Knust, Climate change affects marine fishes through the oxygen limitation of thermal tolerance. *Science* **315**, 95–97 (2007).
10. C. D. G. Harley, A. Randall Hughes, K. M. Hultgren, B. G. Miner, C. J. B. Sorte, C. S. Thornber, L. F. Rodriguez, L. Tomanek, S. L. Williams, The impacts of climate change in coastal marine systems. *Ecol. Lett.* **9**, 228–241 (2006).
11. V. Chaidez, D. Dreano, S. Agusti, C. M. Duarte, I. Hoteit, Decadal trends in Red Sea maximum surface temperature. *Sci. Rep.* **7**, 8144 (2017).
12. J.-P. Truchot, A. Duhamel-Jouve, Oxygen and carbon dioxide in the marine intertidal environment: Diurnal and tidal changes in rockpools. *Respir. Physiol.* **39**, 241–254 (1980).
13. D. Krause-Jensen, N. Marbà, M. Sanz-Martin, I. E. Hendriks, J. Thyrring, J. Carstensen, M. K. Sejr, C. M. Duarte, Long photoperiods sustain high pH in Arctic kelp forests. *Sci. Adv.* **2**, e1501938 (2016).
14. F. C. Mark, C. Bock, H. O. Pörtner, Oxygen-limited thermal tolerance in Antarctic fish investigated by MRI and ^{31}P-MRS. *Am. J. Physiol. Regul. Integr. Comp. Physiol.* **283**, R1254–R1262 (2002).
15. W. C. E. P. Verberk, R. S. E. W. Leuven, G. van der Velde, F. Gabel, Thermal limits in native and alien freshwater peracarid Crustacea: The role of habitat use and oxygen limitation. *Funct. Ecol.* **32**, 926–936 (2018).
16. H.-O. Pörtner, M. K. Grieshaber, in *The Vertebrate Gas Transport Cascade: Adaptations to Environment and Mode of Life* J. E. P. W. Bicudo, Ed. (CRC Press, Boca Raton FL, 1993), pp. 330–357.
17. N. E. Phillips, A. L. Moran, Oxygen production from macrophytes decreases development time in benthic egg masses of a marine gastropod. *Hydrobiologia* **757**, 251–259 (2015).
18. M. W. Beck, K. L. Heck, K. W. Able, D. L. Childers, D. B. Eggleston, B. M. Gillanders, B. Halpern, C. G. Hays, K. Hoshino, T. J. Minello, R. J. Orth, P. F. Sheriden, M. P. Weinstein, The identification, conservation, and management of estuarine and marine nurseries for fish and invertebrates: A better understanding of the habitats that serve as nurseries for marine species and the factors that create site-specific variability in nursery quality will improve conservation and management of these areas. *Bioscience* **51**, 633–641 (2001).
19. C. M. Duarte, I. J. Losada, I. E. Hendriks, I. Mazarrasa, N. Marbà, The role of coastal plant communities for climate change mitigation and adaptation. *Nat. Clim. Change* **3**, 961–968 (2013).
20. I. E. Hendriks, Y. S. Olsen, L. Ramajo, L. Basso, A. Steckbauer, T. S. Moore, J. Howard, C. M. Duarte, Photosynthetic activity buffers ocean acidification in seagrass meadows. *Biogeosciences* **11**, 333–346 (2014).
21. M. Sheaves, R. Baker, I. Nagelkerken, R. M. Connolly, True value of estuarine and coastal nurseries for fish: Incorporating complexity and dynamics. *Estuaries Coasts* **38**, 401–414 (2015).
22. E. B. Barbier, S. D. Hacker, C. Kennedy, E. W. Koch, A. C. Stier, B. R. Siliman, The value of estuarine and coastal ecosystem services. *Ecol. Monogr.* **81**, 169–193 (2011).
23. J. B. Lamb, J. A. J. M. van de Water, D. G. Bourne, C. Altier, M. Y. Hein, E. A. Fiorenza, N. Abu, J. Jompa, C. D. Harvell, Seagrass ecosystems reduce exposure to bacterial pathogens of humans, fishes, and invertebrates. *Science* **355**, 731–733 (2017).
24. D. Breitburg, L. A. Levin, A. Oschlies, M. Grégoire, F. P. Chavez, D. J. Conley, V. Garçon, D. Gilbert, D. Gutiérrez, K. Isensee, G. S. Jacinto, K. E. Limburg, I. Montes, S. W. A. Naqvi, G. C. Pitcher, N. N. Rabalais, M. R. Roman, K. A. Rose, B. A. Seibel, M. Telszewski, M. Yasuhara, J. Zhang, Declining oxygen in the global ocean and coastal waters. *Science* **359**, eaam7240 (2018).
25. J. Z. Sippo, D. T. Maher, D. R. Tait, C. Holloway, I. R. Santos, Are mangroves drivers or buffers of coastal acidification? Insights from alkalinity and dissolved inorganic carbon export estimates across a latitudinal transect. *Global Biogeochem Cy.* **30**, 753–766 (2016).
26. L. Kapsenberg, G. E. Hofmann, Ocean pH time-series and drivers of variability along the northern Channel Islands, California, USA. *Limnol. Oceanogr.* **61**, 953–968 (2016).
27. F. Giomi, C. Mandaglio, M. Ganmanee, G.-D. Han, Y.-W. Dong, G. A. Williams, G. Sarà, The importance of thermal history: Costs and benefits of heat exposure in a tropical, rocky shore oyster. *J. Exp. Biol.* **219**, 686–694 (2016).
28. S. Cannicci, F. Dahdouh-Guebas, A. Diyane, M. Vannini, Natural diet and feeding habits of *Thalamita crenata* (Decapoda: Portunidae). *J. Crustac. Biol.* **16**, 678–683 (1996).
29. L. Fishelson, Ecology and distribution of the benthic fauna in the shallow waters of the Red Sea. *Mar. Biol.* **10**, 113–133 (1971).
30. M. Vannini, G. Innocenti, Research on the coast of Somalia. Portunidae (Crustacea Brachyura). *Trop. Zool.* **13**, 251–298 (2000).
31. T. B. Atwood, R. M. Connolly, E. G. Ritchie, C. E. Lovelock, M. R. Heithaus, G. C. Hays, J. W. Fourqurean, P. I. Macreadie, Predators help protect carbon stocks in blue carbon ecosystems. *Nat. Clim. Change* **5**, 1038–1045 (2015).
32. M. Fusi, F. Giomi, S. Babbini, D. Daffonchio, C. D. McQuaid, F. Porri, S. Cannicci, Thermal specialization across large geographical scales predicts the resilience of mangrove crab populations to global warming. *Oikos* **124**, 784–795 (2015).
33. J. S. Terblanche, A. A. Hoffmann, K. A. Mitchell, L. Rako, P. C. le Roux, S. L. Chown, Ecologically relevant measures of tolerance to potentially lethal temperatures. *J. Exp. Biol.* **10**, 3713–3725 (2011).
34. B. De Wachter, F. J. Sartoris, H. O. Pörtner, The anaerobic end product lactate has a behavioural and metabolic signalling function in the shore crab. *J. Exp. Biol.* **200**, 1015–1024 (1997).
35. P. Greenaway, C. A. Farrelly, The venous system of the terrestrial *crab Ocypode cordimanus* (Desmarest 1825) with particular reference to the vasculature of the lungs. *J. Morphol.* **181**, 133–142 (1984).
36. M. K. Grieshaber, U. Kreutzer, H. O. Pörtner, Critical PO_2 of euryoxic animals. *Oxyg. Sens. Tissues* **1988**, 37–48 (1988).
37. U.S. Geological Survey (USGS) Office of Water Quality Technical Memorandum 2011.03 (2011).
38. C. J. Monaco, C. D. McQuaid, D. J. Marshall, Decoupling of behavioural and physiological thermal performance curves in ectothermic animals: A critical adaptive trait. *Oecologia* **185**, 583–593 (2017).
39. R: A language and environment for statistical computing. Team R Core Vienna Austria. *R Found. Stat. Comput.* (2017); www.R-project.org/.

Acknowledgments: We thank S. Umer for the invaluable support during laboratory work. We are grateful to A. Bodega Martinez for the species illustrations in Fig. 2. We thank M. Hay and two anonymous reviewers whose suggestions helped improve and clarify the early version of the manuscript. **Funding:** This research was funded by KAUST through baseline funding to C.M.D. and D.D.; the Competitive Center Funding 2017–2018, "Role of oxygen availability in shaping the bacterial microbiome of mangrove animal ectotherm species"; and the Competitive Research Grant (CRG-7-3739) to D.D., "The role of the bacterial symbiome at the gill-water (air) interface in the evolution towards terrestrialization (Microlanding)," 1 April 2019 to 31 March 2022. **Author contributions:** F.G. and M.F. designed the study. F.G., J.B., D.D., and M.F. performed the fieldwork. C.M.D., V.S., S.A., and A.A. performed environmental logging measurements. F.G., M.F., A.B., and C.M.D. analyzed and interpreted the results. F.G. and M.F. wrote the first draft of the manuscript. All authors contributed substantially to the final manuscript. **Competing interests:** The authors declare that they have no competing interests. **Data and materials availability:** All data needed to evaluate the conclusions in the paper are present in the paper and/or the Supplementary Materials. Additional data related to this paper may be requested from the authors.

Submitted 28 February 2019
Accepted 7 August 2019
Published 4 September 2019
10.1126/sciadv.aax1814

Citation: F. Giomi, A. Barausse, C. M. Duarte, J. Booth, S. Agusti, V. Saderne, A. Anton, D. Daffonchio, M. Fusi, Oxygen supersaturation protects coastal marine fauna from ocean warming. *Sci. Adv.* **5**, eaax1814 (2019).

Oxygen supersaturation protects coastal marine fauna from ocean warming

Folco Giomi, Alberto Barausse, Carlos M. Duarte, Jenny Booth, Susana Agusti, Vincent Saderne, Andrea Anton, Daniele Daffonchio and Marco Fusi

Sci Adv **5** (9), eaax1814.
DOI: 10.1126/sciadv.aax1814